


Self-Consistent Correlations of Randomly Coupled Rotators in the Asynchronous State

Alexander van Meegen* and Benjamin Lindner

*Bernstein Center for Computational Neuroscience Berlin, Philippstraße 13, Haus 2, 10115 Berlin, Germany
and Physics Department of Humboldt University Berlin, Newtonstraße 15, 12489 Berlin, Germany*

 (Received 14 November 2017; revised manuscript received 9 October 2018; published 20 December 2018)

We study a network of unidirectionally coupled rotators with independent identically distributed (i.i.d.) frequencies and i.i.d. coupling coefficients. Similar to biological networks, this system can attain an asynchronous state with pronounced temporal autocorrelations of the rotators. We derive differential equations for the self-consistent autocorrelation function that can be solved analytically in limit cases. For more involved scenarios, its numerical solution is confirmed by simulations of networks with Gaussian or sparsely distributed coupling coefficients. The theory is finally generalized for pulse-coupled units and tested on a standard model of computational neuroscience, a recurrent network of sparsely coupled exponential integrate-and-fire neurons.

DOI: 10.1103/PhysRevLett.121.258302

When studying large networks of oscillatory elements such as the spiking nerve cells in the brain, pacemaker cells in the heart, or the biochemically and biomechanically interacting cells in developing tissue, research often focuses on collective phenomena like synchronization [1] and global oscillations and waves [2]. However, the emergence of asynchronous irregular activity instead of some form of macroscopic order is frequently more typical, e.g., in the awake behaving animal [3,4] and in corresponding models [5–8]. Understanding the rich temporal structure of the asynchronous state remains an open challenge.

In the asynchronous state, units behave quasistochastically because they are driven by a large number of other (likewise quasistochastic) units. The correlation statistics of the driving, i.e., the colored network noise, is connected to the statistics of the single unit in a self-consistent manner [9–11]. The temporal structure of the network noise is often much richer than suggested by the Poisson noise approximation that is frequently employed in theoretical studies. Temporal correlations depend in nontrivial ways on both the oscillator and network properties and these dependencies are poorly understood.

Analytical progress has been achieved for random networks of rate units (starting with Sompolinsky *et al.* [12] and extended to heterogeneous situations in [13–15]) and for stochastic units with a high level of intrinsic noise for which linear response theory can be applied [16–18]. Studies of deterministic networks of spiking neurons, largely restricted to numerical simulations, found more involved collective dynamics [19–21] and observed long transients and slow fluctuations [8,22–24].

The long-standing challenge for the theory of the asynchronous state is to determine the autocorrelations of the single units and the total network noise. In this paper we tackle this problem for a network of phase oscillators,

derive differential equations for the self-consistent autocorrelation function and solve them in some simple cases. We also generalize the theory to networks of pulse-coupled units and compute approximate power spectra for recurrent networks of integrate-and-fire neurons, an important model class in computational neuroscience.

Model.—We consider a network of $N \gg 1$ unidirectionally coupled rotators, inspired by the asymmetric coupling in neural networks. The state of rotator m is described by its position on the complex unit circle $x_m = \exp(i\Theta_m)$, where Θ_m is a continuous phase variable. This phase variable obeys the dynamical equation

$$\dot{\Theta}_m = \omega_m + \sum_{n \neq m} K_{mn} f(\Theta_n), \quad (1)$$

where ω_m describes the natural frequency of rotator m ; the coupling coefficient K_{mn} and the 2π -periodic function $f(\Theta_n)$ characterize the effect of rotator n on rotator m (with a uniform phase response curve of rotator m). Both the natural frequencies and the coupling coefficients are independent identically distributed (i.i.d.) random variables with $\langle \omega_m \rangle_\omega = \omega_0$, $\langle \Delta \omega_m^2 \rangle_\omega = \sigma_\omega^2$, $\langle K_{mn} \rangle_K = \bar{K}/N$ and $\langle \Delta K_{mn}^2 \rangle_K = K^2/N < \infty$. The coupling is in general not symmetric, i.e., $K_{mn} \neq K_{nm}$. The complete independence of the interaction term of the *driven* phase Θ_m , which makes our model very different to the Kuramoto model and other network models of weakly coupled phase oscillators [25], is certainly a simplifying assumption.

Theory.—In a stochastic mean-field approximation the rotators are driven by temporally correlated but independent Gaussian noise processes $\xi_m(t)$,

$$\dot{\Theta}_m = \omega_m + \xi_m(t). \quad (2)$$

The mean $\langle \xi_m(t) \rangle_\xi = \mu_\xi(t)$ and correlation function $\langle \xi_m(t) \xi_n(t') \rangle_\xi - \langle \xi_m(t) \rangle_\xi \langle \xi_n(t') \rangle_\xi = \delta_{mn} C_\xi(t, t')$ obey

$$\begin{aligned} \mu_\xi(t) &= \bar{K} \langle f(\Theta(t)) \rangle_{\xi, \omega} \\ C_\xi(t, t') &= K^2 \langle f(\Theta(t)) f(\Theta(t')) \rangle_{\xi, \omega}, \end{aligned} \quad (3)$$

where we dropped the indices because they are redundant. Thus, the system of N coupled ordinary differential equations is equivalent to a one-dimensional self-consistent stochastic equation with colored noise. The approximate dynamics [Eqs. (2) and (3)] seems intuitive when regarding the rhs of the original dynamics [Eq. (1)] as a noisy input; their rigorous derivation is based on a dynamical mean-field theory that becomes exact for $N \rightarrow \infty$ (for a similar approach, see [12,26–28]). Briefly, the theory's starting point is the system's generating functional that is averaged over the disorder (distributed coupling coefficients and natural frequencies), decoupled by a Hubbard-Stratonovich transformation and evaluated in a saddle-point approximation (details in Supplemental Material [29], which includes Refs. [30–33]).

We assume a stationary state, in which the auto-correlation function of the Gaussian process $C_\xi(\tau) = \lim_{t_0 \rightarrow \infty} C_\xi(t_0, t_0 + \tau)$ depends only on the time difference τ . With the assumption of invariance under a rotation of the reference frame $\Theta \rightarrow \Theta + \alpha$, we can evaluate Eq. (3) to arrive at a single self-consistent equation [29],

$$C_\xi(\tau) = K^2 \sum_{\ell=-\infty}^{\infty} |A_\ell|^2 \phi(\ell\tau) \exp\left(-\ell^2 \int_0^\tau du (\tau-u) C_\xi(u)\right). \quad (4)$$

Here, we used $f(\Theta) = \sum_{\ell=-\infty}^{\infty} A_\ell e^{i\ell\Theta}$ with $A_\ell^* = A_{-\ell}$, the characteristic function of the natural frequencies $\phi(x) = \langle e^{i\omega x} \rangle_\omega$ and rescaled $\omega_0 + \mu_\xi \rightarrow \omega_0$. To solve Eq. (4) numerically, we rewrite it as an ordinary differential equation for $\Lambda(\tau) = \int_0^\tau du (\tau-u) C_\xi(u)$,

$$\ddot{\Lambda} = K^2 \sum_{\ell=-\infty}^{\infty} |A_\ell|^2 \phi(\ell\tau) \exp[-\ell^2 \Lambda], \quad (5)$$

with initial conditions $\Lambda(0) = \dot{\Lambda}(0) = 0$. Equation (5) is straightforward to solve numerically for a finite number of Fourier coefficients A_ℓ and yields the autocorrelation function of the input via

$$C_\xi(\tau) = K^2 \sum_{\ell=-\infty}^{\infty} |A_\ell|^2 \phi(\ell\tau) \exp[-\ell^2 \Lambda(\tau)]. \quad (6)$$

The stationary autocorrelation function of a rotator $C_{x_m}(\tau) = \lim_{t_0 \rightarrow \infty} \langle x_m^*(t_0) x_m(t_0 + \tau) \rangle_\xi$ follows from

$$C_{x_m}(\tau) = \langle e^{i \int_0^\tau du \dot{\Theta}_m(u)} \rangle_\xi = \exp[i\omega_m \tau - \Lambda(\tau)]. \quad (7)$$

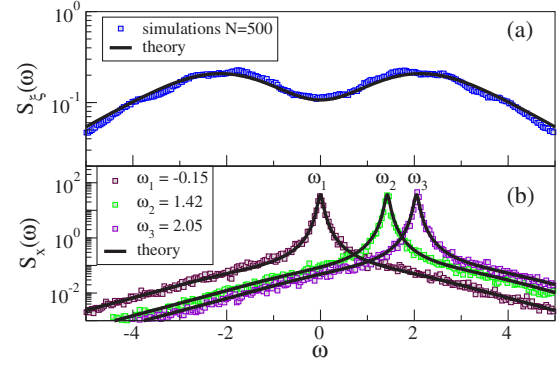


FIG. 1. System with distributed natural frequencies. Noise spectrum (a) and spectra of three arbitrarily picked oscillators (b) with natural frequencies as indicated; network simulations (squares) compared to theory (lines) obtained from numerically solving Eq. (5) and Fourier transformation of Eqs. (6) and (7), respectively. Parameters: Gaussian coupling coefficients, $\bar{K} = 0$, $K = 0.5$, $\omega_0 = 1$, $\sigma_\omega = 0.5$, $A_2 = 1/2$, $A_3 = 1/2i$, $A_\ell = 0$ otherwise. In simulations, we used a time step of $\Delta t = 0.1$ a.u. in a time window of $T = 26T_0$, discarded a transient of $T_0 = 2500$ a.u. and used the remaining 25 pieces of length T_0 for averaging.

Because we deal with oscillatory functions, it is more convenient to consider the respective power spectra, $S_{\{x, \xi\}}(\omega) = \int_{-\infty}^{\infty} d\tau e^{-i\omega\tau} C_{\{x, \xi\}}(\tau)$, obtained by Fourier transformation of the various correlation functions (in all simulated spectra, we omit the dc component).

Examples with higher-mode interactions.—To test the theory, we first select a case with a broad Gaussian distribution of natural frequencies, an interaction function with two Fourier modes [$f(\Theta) = \cos(2\Theta) + \sin(3\Theta)$] and a moderately sized network of 500 rotators (Fig. 1). The noise spectrum is rather broad [Fig. 1(a)], whereas the single rotator spectra are strongly peaked and located at the (here arbitrarily selected) natural frequencies [Fig. 1(b)]. Network simulations fully confirm our theory.

The temporal correlations become more structured if we do not distribute natural frequencies ($\sigma_\omega = 0$), while keeping all other parameters the same as before (Fig. 2). From our theory it becomes apparent why the specific choice of two Fourier modes leads to pronounced peaks at $|\omega| = 2\omega_0$ and $|\omega| = 3\omega_0$ in the noise spectrum [arrows in Fig. 2(a)]. These peaks show up as well in the spectra of the single rotators [arrows in Fig. 2(b)] at $\omega = (1 \pm 2)\omega_0$ and at $\omega = (1 \pm 3)\omega_0$ and, together with the peak at ω_0 , form a rich correlation structure that is in all details accounted for by our theory.

As our theory has been developed for large N , a small discrepancy between theory and simulations emerges for $N = 50$ around the main spectral peak [cf., Fig. 2(c)]. In Fig. 2(d) we plot the relative deviation $\Delta = \int_{-\omega_{\text{Nyquist}}}^{\omega_{\text{Nyquist}}} d\omega (S_x^{\text{theo.}}(\omega) - \langle S_x^{\text{simul.}}(\omega) \rangle_N)^2 / \int_{-\omega_{\text{Nyquist}}}^{\omega_{\text{Nyquist}}} d\omega \langle S_x^{\text{simul.}}(\omega) \rangle_N^2$, where $\langle \cdot \rangle_N$ denotes an average over the rotators as a function of N . Indeed, Δ drops with N and becomes small

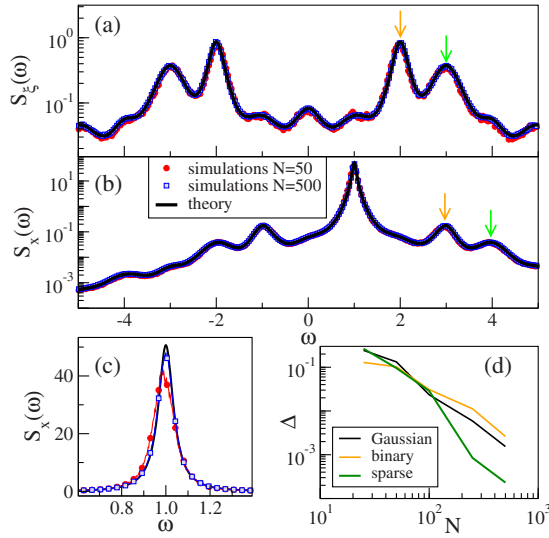


FIG. 2. System with a single natural frequency. Spectra of noise (a) and single-rotator (b), averaged over all units (b) for two system sizes as indicated. Network simulations (squares) compared to theory (lines) [expanded view in (c)]. Deviation Δ between theory and simulations for the (network-wide averaged) single-rotator spectrum for different connectivities (d). Parameters as in Fig. 1 except $\sigma_\omega = 0$.

for a few hundred units already. In the same graph we not only show results for the so-far-used Gaussian connectivity but also for a binary distribution (K_{mn} are randomly picked from $\{-K/\sqrt{N}, K/\sqrt{N}\}$) and for a sparse connectivity with vanishing mean value (K_{mn} come from $\{-K/\sqrt{Np(1+p/q)}, 0, K/\sqrt{Nq(1+q/p)}\}$ with probabilities $p = 0.02, 1-p-q, q = 0.08$, mimicking the sparse connections in neural networks). In all cases, the agreement between theory and network simulations systematically improves with growing N and, remarkably, is best for the biologically realistic sparse case. For the remainder, we keep the sparse connectivity.

Analytically tractable example.—The parameter space of the model is large. Here, we focus on a simple case that allows for an analytical treatment: The frequencies are not distributed ($\sigma_\omega = 0$) and the coupling function is $f(\Theta_m) = \sin(\Theta_m)$, leading in Eq. (5) to $\tilde{\Lambda} = (K^2/2) \cos(\omega_0\tau) e^{-\Lambda}$. As we can rescale time with the natural frequency ω_0 , this leaves one parameter K/ω_0 . We proceed with the two limiting cases $\omega_0 \ll K$ and $\omega_0 \gg K$ and focus on the single rotator [the noise autocorrelation is simply $C_\xi(\tau) = (K^2/2) \text{Re}(C_x(\tau))$]; detailed derivations are in [29].

For sufficiently small ω_0 ($\omega_0 \ll K$), we obtain

$$C_x(\tau) \approx \frac{\exp(i\omega_0\tau)}{\cosh^2(K\tau/2)}, \quad S_x(\omega) \approx \frac{4\pi(\omega - \omega_0)/K^2}{\sinh(\pi(\omega - \omega_0)/K)}. \quad (8)$$

The quality factor $Q_x = \omega_0/\Delta\omega$ with $\Delta\omega$ being the full width of the peak at half maximum can be calculated as

$$Q_x \approx \frac{\pi\omega_0}{2zK}, \quad \text{where } z = \sinh(z)/2 \approx 2.17732. \quad (9)$$

The correlation time of the rotators reads

$$\tau_x = \int_0^\infty d\tau \left| \frac{C_x(\tau)}{C_x(0)} \right| \approx \frac{2}{K}, \quad (10)$$

while the intensity of the network noise is given by

$$D_\xi = \int_0^\infty d\tau |C_\xi(\tau)| \approx K, \quad (11)$$

where we used the definitions proposed in Ref. [34] and both results become exact for $\omega_0 = 0$.

In the opposite limit of a very large natural frequency, we obtain

$$C_x(\tau) \approx \frac{\exp(i\omega_0\tau)}{\cosh(K^2\tau/(2\sqrt{2}\omega_0))},$$

$$S_x(\omega) \approx \frac{2\sqrt{2}\pi\omega_0/K^2}{\cosh(\sqrt{2}\pi\omega_0(\omega - \omega_0)/K^2)}. \quad (12)$$

For the correlation time, noise intensity and quality factor follow for $K \ll \omega_0$,

$$Q_x \approx \frac{\pi\omega_0^2/K^2}{\sqrt{2}|\cosh^{-1}(2)|}, \quad \tau_x \approx \frac{\sqrt{2}\pi\omega_0}{K^2}, \quad D_\xi \approx \sqrt{2}\omega_0. \quad (13)$$

Equations (8)–(13) agree well with simulation results (Fig. 3). As illustrated in Fig. 3(a) [Fig. 3(b)], a weak (strong) coupling strength leads to a sharp (broad) spectral peak at the natural frequency. Similarly, the quality factor [Fig. 3(c)], the correlation time [Fig. 3(d)], and the network noise intensity [Fig. 3(e)] show a good agreement valid beyond the strict asymptotic regimes $K \ll \omega_0$ and $K \gg \omega_0$.

Application to a recurrent network of spiking neurons.—With a small modification, our theory is applicable to the self-consistent autocorrelation statistics of spiking neurons in sparse recurrent networks (details in [29] including Refs. [35,36]). Choosing a Dirac comb for $f(\Theta)$ that is multiplied by the time derivative of the input unit, i.e., changing the model to

$$\dot{\Theta}_m = \omega_m + \sum_{n \neq m} K_{mn} \dot{\Theta}_n \sum_{k=-\infty}^{\infty} \delta(\Theta_n - 2\pi k), \quad (14)$$

we can mimic the spikes arising from threshold crossings in the conventional integrate-and-fire (IF) neuron. To make the Dirac delta distribution numerically tractable, we regularize it as $\delta(x) \rightarrow (1/\sqrt{2\pi\lambda^2}) \exp(-x^2/2\lambda^2)$ with $\lambda \ll 2\pi$. This leads to the self-consistency equation

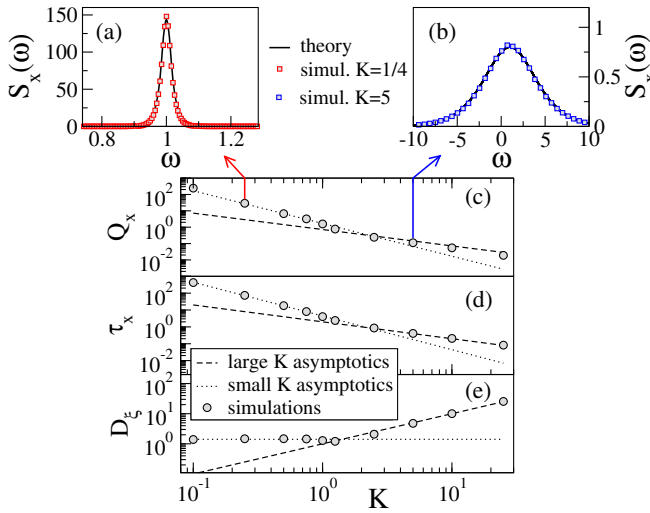


FIG. 3. Analytically tractable cases. Power spectra for weak (a) and strong (b) coupling strength; theory [lines, Eqs. (12) and (8), respectively] compared to network simulations (symbols). Quality factor (c), correlation time (d) of rotators and network noise intensity (e); theory [lines, Eqs. (9)–(11) and (13)] and simulations (symbols). Parameters: See Fig. 2 except $A_1 = A_{-1}^* = 1/2i$, $A_\ell = 0$, $T_0 = 5000$ a.u..

$$\begin{aligned} \ddot{\Lambda} = \frac{K^2}{4\pi^2} & \left\{ (\ddot{\Lambda} + \sigma_\omega^2 + \omega_0^2) \vartheta_3 \left[\frac{1}{2} \omega_0 \tau, e^{-\frac{1}{2} \sigma_\omega^2 \tau^2 - \lambda^2 - \Lambda} \right] \right. \\ & + \omega_0 (\sigma_\omega^2 \tau + \dot{\Lambda}) \vartheta_3' \left[\frac{1}{2} \omega_0 \tau, e^{-\frac{1}{2} \sigma_\omega^2 \tau^2 - \lambda^2 - \Lambda} \right] \\ & \left. + \frac{1}{4} (\sigma_\omega^2 \tau + \dot{\Lambda})^2 \vartheta_3'' \left[\frac{1}{2} \omega_0 \tau, e^{-\frac{1}{2} \sigma_\omega^2 \tau^2 - \lambda^2 - \Lambda} \right] \right\}, \quad (15) \end{aligned}$$

where $\vartheta_3(z, q) = \sum_{\ell=-\infty}^{\infty} e^{2i\ell z} q^{\ell^2}$ denotes the Jacobi Theta function, $\vartheta_3^{(n)}(z, q) = \partial_z^n \vartheta_3(z, q)$, and we rescaled $\omega_0 + \mu_\xi \rightarrow \omega_0$ with $\mu_\xi = \bar{K} \omega_0 / (2\pi - \bar{K})$.

We compare the resulting spectra of network noise and single unit to simulation results of a sparse heterogeneous network of N_E excitatory and N_I inhibitory EIF neurons governed by

$$\tau_m \dot{V}_i = -(V_i - V_{\text{leak}}) + \Delta_T e^{-\frac{V_i - V_{\text{th}}}{\Delta_T}} + RI_i(t) \quad (16)$$

supplemented by the fire-and-reset rule; i.e., whenever the voltage diverges (or, in the simulations, reaches a threshold V_{peak}) a spike is registered and the voltage is reset to V_{reset} and kept constant during the refractory period t_{ref} . The total recurrent input $RI_i(t) = RI_{\text{ext},i} + \tau_m J_E \sum_{j \in N_E} C_{ij} x_j(t - \tau_D) + \tau_m J_I \sum_{j \in N_I} C_{ij} x_j(t - \tau_D)$ consists of the excitatory (inhibitory) recurrent contributions with amplitudes J_E ($J_I = -gJ_E$), where $x_i(t) = \sum_k \delta(t - t_i^k)$ denotes the spike train of neuron i , τ_D is the transmission delay, and C_{ij} is a random connectivity matrix with i.i.d. distributed entries that are 1 with probability ε and 0 otherwise. An important

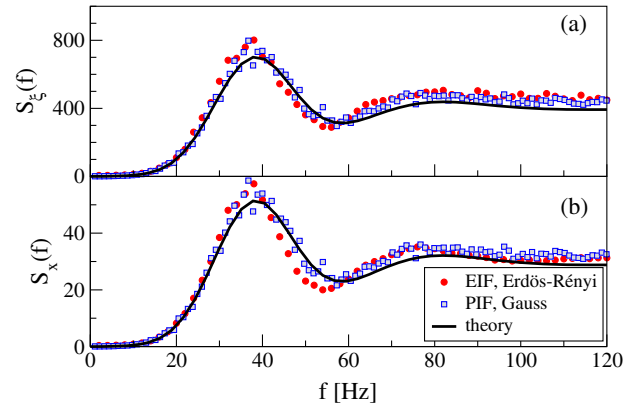


FIG. 4. Application to neural network model. Noise spectrum (a) and spectrum of the single neuron spike train, averaged over all units (b). Network simulations of exponential integrate-and-fire (EIF) neurons with Erdős-Rényi topology obeying Dale's law (circles), perfect integrate-and-fire (PIF) neurons with fully connected Gaussian topology (squares) compared to the theory (lines). Parameters: $N_E = 10000$, $N_I = 2500$, $\varepsilon = 0.1$, $J_E = 0.05$ mV, $g = 4.5$, $RI_{\text{ext}} = 30$ mV, $\sigma_{\text{ext}} = 0.1RI_{\text{ext}}$, $V_{\text{th}} = 20$ mV, $V_{\text{leak}} = 0$ mV, $V_{\text{reset}} = 0$ mV, $\Delta_T = 2$ mV, $\tau_m = 20$ ms, $t_{\text{ref}} = 2$ ms, $\tau_D = 1.5$ ms, $\lambda = 0.08$, $dt = 0.1$ ms, $T_0 = 1$ s, and $T = 11T_0$.

biophysical constraint is given by Dale's law; i.e., excitatory neurons form only excitatory outgoing connections and vice versa for inhibitory neurons. Cell-to-cell variability is implemented by means of a constant input current to each neuron that is drawn from a Gaussian distribution with mean RI_{ext} and variance σ_{ext}^2 (corresponding to the distribution of natural frequencies in the rotator network). This type of network is frequently used in computational neuroscience to study the asynchronous irregular state of cortical networks [6,8,24]. Deep in the mean-driven regime of the spiking network, the spectra obtained from solving the modified rotator Eq. (15) display a good agreement with the spectra of the network noise [Fig. 4(a)] and the single-neuron's spike train [Fig. 4(b)] obtained from simulating the spiking network using the NEST simulator [37].

Conclusions.—In this Letter we explored the emergence of a dynamical network noise in a random network of deterministic phase oscillators. We obtained equations for the second-order temporal correlation statistics, which are formally exact in the limit $N \rightarrow \infty$. Focusing on an analytically tractable case, we derived asymptotic solutions for the stationary autocorrelation functions of the network fluctuations and the rotators, respectively. Furthermore, we generalized the theory to the important case of a recurrent neural network of spiking neurons and demonstrated that our rotator-network theory is applicable if the integrate-and-fire neurons are in a strongly mean-driven regime. It is still an open problem how the autocorrelation of IF neurons can be calculated when the model operates in the fluctuation-driven regime where our rotator approximation fails.

Our work paves the way for more detailed studies of how the statistics of connection strength, the network's heterogeneity, and the interaction function shape the network noise and the autocorrelations of the single element if this element has an predominantly oscillatory nature. Mathematically, it is an interesting challenge to prove the stability of the asynchronous state of our model under general conditions. Furthermore, it is plausible but has to be worked out in detail whether interactions of distinct oscillator populations may be described by separate but coupled equations for the different correlation functions. Another exciting topic for future research is the response of our model to external stimuli and the accompanying change of the correlation statistics. Finally, a theoretical understanding of power spectra of weighted sums of the synaptic input (like the network noise) in spiking neural networks enables systematic studies of rhythms in the local field potential [2], an experimentally accessible quantity arising from filtered synaptic input currents [38,39].

We thank Davide Bernardi, Alexander Neiman, and Misha Zaks for valuable comments on an earlier version of this Letter.

*avm@physik.hu-berlin.de

- [1] A. Pikovsky, M. Rosenblum, and J. Kurths, *Synchronization: A Universal Concept in Nonlinear Sciences* (Cambridge University Press, Cambridge, England, 2001).
- [2] G. Buzsáki, *Rhythms of the Brain* (Oxford University Press, New York, Oxford, 2006).
- [3] J. F. A. Poulet and C. C. H. Petersen, *Nature (London)* **454**, 881 (2008).
- [4] K. D. Harris and A. Thiele, *Nat. Rev. Neurosci.* **12**, 509 (2011).
- [5] C. van Vreeswijk and H. Sompolinsky, *Science* **274**, 1724 (1996).
- [6] A. Renart, J. D. L. Rocha, P. Bartho, L. Hollender, N. Parga, A. Reyes, and K. D. Harris, *Science* **327**, 587 (2010).
- [7] M. Helias, T. Tetzlaff, and M. Diesmann, *PLoS Comput. Biol.* **10**, e1003428 (2014).
- [8] S. Ostojic, *Nat. Neurosci.* **17**, 594 (2014).
- [9] A. Lerchner, G. Sterner, J. Hertz, and M. Ahmadi, *Netw. Comput. Neural Syst.* **17**, 131 (2006).
- [10] B. Dummer, S. Wieland, and B. Lindner, *Front. Comput. Neurosci.* **8**, 104 (2014).
- [11] R. Pena, S. Vellmer, D. Bernardi, A. Roque, and B. Lindner, *Front. Comput. Neurosci.* **12**, 9 (2018).
- [12] H. Sompolinsky, A. Crisanti, and H. J. Sommers, *Phys. Rev. Lett.* **61**, 259 (1988).
- [13] J. Aljadeff, M. Stern, and T. Sharpee, *Phys. Rev. Lett.* **114**, 088101 (2015).
- [14] J. Kadmon and H. Sompolinsky, *Phys. Rev. X* **5**, 041030 (2015).
- [15] F. Mastrogiuseppe and S. Ostojic, *PLoS Comput. Biol.* **13**, e1005498 (2017).
- [16] V. Pernice, B. Staude, S. Cardanobile, and S. Rotter, *PLoS Comput. Biol.* **7**, e1002059 (2011).
- [17] J. Trousdale, Y. Hu, E. Shea-Brown, and K. Josic, *PLoS Comput. Biol.* **8**, e1002408 (2012).
- [18] D. Grytskyy, T. Tetzlaff, M. Diesmann, and M. Helias, *Front. Comput. Neurosci.* **7**, 131 (2013).
- [19] M. Monteforte and F. Wolf, *Phys. Rev. X* **2**, 041007 (2012).
- [20] E. Ullner and A. Politi, *Phys. Rev. X* **6**, 011015 (2016).
- [21] E. Ullner, A. Politi, and A. Torcini, *Chaos* **28**, 081106 (2018).
- [22] R. Zillmer, N. Brunel, and D. Hansel, *Phys. Rev. E* **79**, 031909 (2009).
- [23] B. Kriener, H. Enger, T. Tetzlaff, H. E. Plesser, M.-O. Gewaltig, and G. T. Einevoll, *Front. Comput. Neurosci.* **8**, 136 (2014).
- [24] S. Wieland, D. Bernardi, T. Schwalger, and B. Lindner, *Phys. Rev. E* **92**, 040901(R) (2015).
- [25] F. C. Hoppensteadt and E. M. Izhikevich, *Weakly Connected Neural Networks* (Springer-Verlag, New York, 1997).
- [26] H. Sompolinsky and A. Zippelius, *Phys. Rev. B* **25**, 6860 (1982).
- [27] J. C. Stiller and G. Radons, *Phys. Rev. E* **58**, 1789 (1998).
- [28] J. Schuecker, S. Goedeke, D. Dahmen, and M. Helias, [arXiv:1605.06758](https://arxiv.org/abs/1605.06758).
- [29] See Supplemental Material at <http://link.aps.org/supplemental/10.1103/PhysRevLett.121.258302> for detailed derivations and further information.
- [30] H. Kleinert, *Path Integrals in Quantum Mechanics, Statistics, Polymer Physics, and Financial Markets* (World Scientific, New Jersey, 2009).
- [31] R. L. Stratonovich, in *Noise in Nonlinear Dynamical Systems* (Cambridge University Press, Cambridge, England, 1989), Vol. 1, pp. 16–71.
- [32] C. De Dominicis, *Phys. Rev. B* **18**, 4913 (1978).
- [33] P. Hänggi, *Z. Phys. B* **75**, 275 (1989).
- [34] P. Hänggi and P. Jung, *Adv. Chem. Phys.* **89**, 239 (1995).
- [35] L. Badel, S. Lefort, R. Brette, C. C. H. Petersen, W. Gerstner, and M. J. E. Richardson, *J. Neurophysiol.* **99**, 656 (2008).
- [36] N. Brunel, *J. Comput. Neurosci.* **8**, 183 (2000).
- [37] M. O. Gewaltig and M. Diesmann, *Scholarpedia* **2**, 1430 (2007).
- [38] G. T. Einevoll, C. Kayser, N. K. Logothetis, and S. Panzeri, *Nat. Rev. Neurosci.* **14**, 770 (2013).
- [39] C. Bedard, H. Kroger, and A. Destexhe, *Phys. Rev. Lett.* **97**, 118102 (2006).